

Gianluca Fossati¹
Pietro Cremonesi¹
Gaetano Izzo¹
Emanuele Rizzi¹
Giovanni Sandrone¹
Stephen Harding²
Neil Errington²
Christopher Walters²
Brian Henderson³
Michael M. Roberts⁴
Anthony R.M. Coates⁴
Paolo Mascagni¹

The *Mycobacterium tuberculosis* Chaperonin 10 Monomer Exhibits Structural Plasticity

¹ Italfarmaco Research Centre,
via Laboratori 54, Cinisello
Balsamo
20092 Milan, Italy

² Department of Applied
Biochemistry and Food
Science,
University of Nottingham,
Nottingham, United Kingdom

³ Cellular Microbiology
Research Group,
Eastman Dental Institute,
University College London,
London, United Kingdom

⁴ Department of Medical
Microbiology, St. George's
Hospital Medical School,
University of London, London,
United Kingdom

Received 26 January 2004;
accepted 6 April 2004

Published online 21 July 2004 in Wiley InterScience (www.interscience.wiley.com).
DOI 10.1002/bip.20106

Abstract: The conditions which favor dissociation of oligomeric *Mycobacterium tuberculosis* chaperonin 10 and the solution structure of the monomer were studied by analytical ultracentrifugation, size exclusion chromatography, fluorescence, and circular dichroism spectroscopies. At neutral pH and in the absence of divalent cations, the protein is fully monomeric below approximately a 4.7 μM concentration. Under these conditions the monomer forms completely unfolded and partially folded conformers which are in equilibrium with each other. One conformer accumulates over the others which is stable within a very narrow range of temperatures. It contains a β -sheet-structured C-terminal half and a mostly disordered N-terminal half. Other components of the equilibrium include partially helical structures which do not completely unfold at high temperature or under strong acidic conditions. Complete unfolding of the monomer occurs in the presence of denaturants or below 14°C. Cold-denaturation is detected at an unusually high temperature and

Correspondence to: Paolo Mascagni, Italfarmaco Research Centre, via Laboratori 54, Cinisello Balsamo 20092 Milan, Italy;
e-mail: p.mascagni@italfarmaco.com

Biopolymers, Vol. 75, 148–162 (2004)
© 2004 Wiley Periodicals, Inc.

this may be due to the concentration of hydrophobic residues, which is larger in chaperonins than in other globular proteins. Finally, the monomer self-associates in the pH range 5.8–2.9, where it forms small oligomers. A structure–activity relationship was investigated with the sequences known to be involved in the various biological activities of the monomer. © 2004 Wiley Periodicals, Inc. Biopolymers 75: 148–162, 2004

INTRODUCTION

Chaperonins (Cpns) are a family of sequence-related proteins that are found in all cellular life forms.¹ They bind nonnative, dysfunctional forms of other proteins and assist them to change into correctly folded structures. The GroE chaperonin folding machine^{2,3} is a large complex of about one million Da. It consists of two stacked rings of seven noncovalently bound 60-kDa subunits (Cpn60) each.^{4–6} The 10-kDa co-chaperonin (Cpn10) also forms noncovalently linked heptamers^{7–11} and in the Cpn60/Cpn10 complex is positioned like a lid on top of the Cpn60 tetradecamer.⁴ Each Cpn10 subunit folds in an irregular β -sheet that has structural similarities to the N-terminal catalytic domains of quinone oxidoreductase, glucose dehydrogenase, and alcohol dehydrogenase, suggesting an evolutionary origin of these domains.¹²

Although refolding of nonnative proteins by chaperonins occurs intracellularly, there are several examples of Cpns being secreted outside the cellular environment.^{13–17} One of these examples is *Mycobacterium tuberculosis* (*M. tuberculosis*) Cpn10, a 99-amino-acid-long chaperonin which has been found outside the intact bacillus in *M. tuberculosis*-infected human macrophages.¹⁸

One question then arises from this observation: Do secreted Cpn10s have biological functions in addition to their capacity to fold proteins?

A number of reports have begun to appear suggesting that chaperonins have other biological functions.¹⁹ For instance, Cpn60 can produce pores in cells²⁰ and can stimulate the synthesis of cytokines.^{21,22} Also, *M. tuberculosis* Cpn60 has recently been reported to induce the expression of the vascular adhesion proteins CD54, CD62E, and CD106 by a cytokine-independent mechanism²³ and human Cpn10 has been claimed to be equivalent to an essential growth factor termed early pregnancy factor.²⁴ We have shown that Cpn60 from *Actinobacillus actinomycetemcomitans* and *Escherichia coli* (*E. coli*) can potently stimulate the resorption of bone in vitro.²⁵ Similarly, we have also shown that Cpn10 from *E. coli* and *M. tuberculosis* can induce bone resorption.²⁶ Bone resorption is a central feature of the pathology of spinal tuberculosis, one of the most debilitating types of disease associated with *M. tuberculosis*. The biological activ-

ities of the chaperonins, with particular regard to their immunopathological actions, have been reviewed recently.²⁷

Thus it is emerging that the chaperonins, once released from cells, have biological actions which probably cause tissue pathology.

A further question that arises from these observations is whether the tetradecameric and heptameric structures, which are the functional species in the chaperoning activity of Cpns, are involved at all in the extra-cellular activities of these proteins or whether other species that arise from their dissociation contribute to these activities.

In secreted Cpn10s, a change in quaternary structure is likely to occur as the protein translocates from within the cell, where its concentration is very high, to the outside, where dilution occurs. Dilution-induced dissociation studies have shown that *E. coli* and human Cpn10s are largely monomeric below about a 0.1 μM concentration and that the dissociation reaction is a highly cooperative process that involves heptamers and monomers only.^{28–32} In contrast, the dissociation of *M. tuberculosis* Cpn10 to monomers is more complex and stable oligomers other than the heptamer have been detected (³³ and P. Mascagni (in preparation)).

A final question deriving from these studies is whether the monomer, which prevails in dilute solutions, plays a role in any of these extra-cellular activities.

The bone resorbing activity of *M. tuberculosis* Cpn10 is maximal at nano- to picomolar concentrations. Under these conditions the protein is likely to be monomeric since Cpn10s fully dissociate to monomers at sub-micromolar concentrations.^{28–32} The apoptotic activity of *M. tuberculosis* Cpn10 is dose-dependent, with a bell-shaped curve and peak activity at 10^{-9} M.³⁴ This suggests that the monomer is the active species at 10^{-9} M and that oligomerization at higher concentrations causes loss of activity. Additional activities attributed to the monomeric form of *M. tuberculosis* Cpn10 include the synthesis of the pro-inflammatory cytokine interleukin-6 by a range of human mesenchymal and myeloid cells (B. Henderson, unpublished observation).

Thus it appears that the monomer may play a role in some of the extra-cellular activities of chaperonins.

In this and related work we began to address some of these questions by studying the mechanisms of dissociation of heptameric *M. tuberculosis* Cpn10 and by performing structural and conformational studies in dilute solutions. In particular, the protein and a number of progressively shorter N-terminal peptides were examined under a variety of different conditions, which included protein concentration, pH and temperature extremes, mixed solvents, and the presence of detergents.^{18,33} Circular dichroism (CD) spectroscopy was used to monitor secondary structure changes while mass spectrometry, analytical ultracentrifugation (AUC), and size exclusion chromatography (SEC) were used to detect changes in the protein quaternary structure. Some of the results from these studies are described elsewhere.^{18,33} Here we show that in phosphate buffer at neutral pH, *M. tuberculosis* Cpn10 is monomeric below approximately a 4.7 μM concentration and that the monomer exists in at least three different conformational states. The first is a fully denatured state that predominates below 14°C (cold-denatured state). The second state exists in a narrow range of temperature (i.e., 14–24°C) and is characterized by the presence of one or more β -sheets at the C-terminus and a mostly disordered N-terminal half. The third state contains stable helices and its concentration increases under conditions that mimic those of the cell membrane.¹⁸ These results are consistent with previous observations showing that the monomers arising from the dissociation of other Cpn10 heptamers are either largely unfolded^{31,35} or are partially folded but only marginally stable at room temperature.^{28,32} We also showed that under moderate acidic conditions, oligomerization is favored and at approximately 0.9 μM the monomer self-associates to oligomers. The secondary structure of these oligomers is similar to that previously described for heptameric and tetrameric *M. tuberculosis* Cpn10,³³ being composed primarily of β -sheets and random coils.

These data add to our previous observations of the existence of various stable oligomeric structures of *M. tuberculosis* Cpn10 and suggest that a correlation between the structural heterogeneity exhibited by this protein and its diverse biological effects exists.

MATERIALS AND METHODS

Peptides and Protein

M. tuberculosis Cpn10 was expressed in *E. coli* as previously described.³³ The shorter peptides were prepared by solid-phase synthesis and purified by HPLC to more than 95% homogeneity.³⁶ In the case of the longer sequences,

purification involved their reversible derivatization using the lipophilic probe [4-dodecylaminocarbonylfluoren-9-yl]-methyl succinimidyl carbonate to separate the correct sequence from peptide impurities by reverse-phase chromatography, as described previously.³⁷

Analytical Ultracentrifugation

Sedimentation equilibrium experiments were performed using an Optima XL-I (Beckman Scientific Inc., Palo Alto, CA, USA) analytical ultracentrifuge employing Rayleigh interference optics for increased sensitivity due to low molecular extinction in the near-uv of the Cpn10 samples. Double sector multichannel cells with optical path lengths of 12 mm were used with solutions in one sector and dialysate in the other. Solution column lengths of 0.25 cm were employed (corresponding to a loading volume of ~ 80 μL). The samples were run overnight at either 30,000 or 40,000 rpm for a total of 26 h, at which stage sedimentation equilibrium had been reached, as confirmed by superposition of successive scans taken 2 h apart. All data were captured and analyzed using MSTARI ultracentrifuge data analysis software.³⁸

Sedimentation velocity was also determined in the XL-I ultracentrifuge using Rayleigh interference optics. Run speed and temperature were set at 50,000 rpm and 20°C, respectively, throughout, with a scan interval of ~ 3 min. All sedimentation coefficients were determined using the time derivative (g (s*) analysis) software DC/DT⁺, version 1.12 (J. Philo, Biotechnology & Software Consulting, Thousand Oaks, CA, USA). All sedimentation coefficients were corrected to standard conditions of the viscosity and density of water at 20°C.

Size Exclusion Chromatography

Experiments were carried out using a Hewlett-Packard 1090 HPLC apparatus and a TSK-G3000 SWXL column (300 \times 7.8 mm) (Toyo Pearl, Japan). Monitoring was at 214 nm and a flow rate of 0.38 mL/min.

Circular Dichroism Spectroscopy

CD measurements were performed using a Jasco J-600 spectropolarimeter calibrated with D-10 camphorsulfonic acid. The cuvette had either a 1-cm path length for dilute protein solutions (i.e., 0.01 mg/mL) or a 0.1-cm path length for all other solutions. Spectra were recorded at 0.1-nm intervals in the range 185–250 nm. They were the average of eight scans collected at 50 nm/min each, with a bandwidth set at 2 nm, and were baseline corrected by subtracting the corresponding blank.

Prior to use, the solutions were equilibrated at the desired temperature for about 0.5 h. The observed ellipticity was converted to mean residue weight ellipticity [Θ]deg.cm².d.mol⁻¹). On some occasions, smoothing of the curves, using a mild function which increased the signal to noise ratio without altering the shape of spectra, was applied

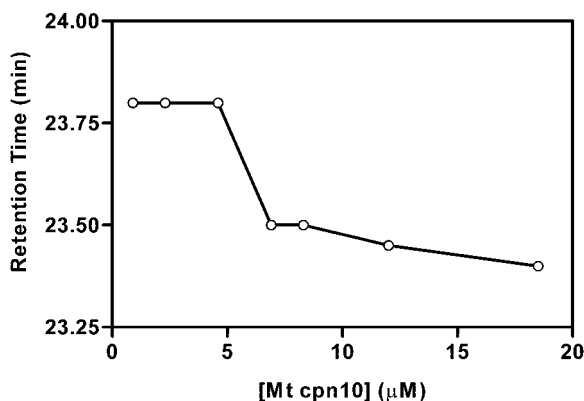


FIGURE 1 Protein concentration dependence of the retention time of *M. tuberculosis* Cpn10 as measured by size exclusion chromatography in 50 mM PO_4^{3-} , pH 7.4, in the concentration range 0.9–18 μM .

using the Jasco J-700 program. Superimposition of smoothed spectra with the raw curve was performed each time to check for artifacts.

Fluorescence Spectroscopy

Fluorimetric measurements were performed with a Jasco FP-6200 spectrofluorimeter in a 3-mL quartz cell using excitation wavelengths of 278 and 295 nm. The emission spectra of protein solutions were recorded between 310 and 390 nm and blank subtracted. The excitation and emission slits were set at 5 and 20 nm, respectively.

RESULTS

Dissociation Studies

To identify the concentration conditions which favor monomeric *M. tuberculosis* Cpn10, sedimentation equilibrium studies were performed in 50 mM PO_4^{3-} , pH 7.4.

At 9.3 μM , the weight-averaged molecular weights of the protein were 30 and 20 kDa at 30,000 and 40,000 rpm, respectively, indicating self-association under these conditions (M_r of the monomer, 10,673 Da). Full dissociation to monomers occurred at a 4.7 μM loading concentration, where the weight-averaged molecular weights were 12 and 11 kDa at the two rotor speeds, respectively.

The complete dissociation of the protein in dilute solutions was confirmed by size exclusion chromatography carried out in the 18–0.9 μM Cpn10 concentration range. At 18 μM , the protein eluted as a single peak at about 23.4 min. Its retention time increased progressively upon dilution, indicating dissociation into smaller species (Figure 1). At 4.7 μM , the reten-

tion time was 23.8 min and did not change upon further dilutions, consistent with the complete dissociation to monomers (Figure 1).

Solution Structure of the *M. tuberculosis* Cpn10 Monomer

The structure of the monomer was studied in dilute protein solutions by a number of different techniques, including sedimentation velocity and fluorescence and CD spectroscopies. Furthermore, a number of progressively shorter synthetic peptides, namely, peptides 26-99, 46-99, 51-99, 54-99, 59-99, 65-99, and 75-99, were used to detect structured regions in the monomer.

Analytical Ultracentrifugation. Preliminary information about the shape of the *M. tuberculosis* Cpn10 monomer was obtained by sedimentation velocity studies, which allowed us to determine the translational frictional coefficient, f , of the molecule and the axial ratio of the equivalent prolate ellipsoid. These two parameters were calculated using the program *ELLIPSI*³⁹ (confirmed by the program *SEDNTERP*⁴⁰) and a value of 0.3 g/g for the hydration of the protein.

At 20°C and a 4 μM loading concentration, the sedimentation coefficient of the *M. tuberculosis* Cpn10 monomer was 1.25 ± 0.25 S, the axial ratio of the equivalent prolate ellipsoid about 5, and the frictional ratio, ff_o , about 1.4, indicating that the monomer is not completely unfolded ($ff_o > 1$) and is elongated in shape (axial ratio $\gg 1$).

Fluorescence Spectroscopy. The existence of folded monomeric structures was confirmed by fluorescence spectroscopy. The sequence of Cpn10 contains five fluorophores, one tryptophan at position 50 (Trp50), and four tyrosines, at positions 70, 73, 80, and 83, respectively. The fluorescence emission spectrum of the monomer obtained by selectively exciting Trp50 at 295 nm, had λ_{max} of about 350 nm (Figure 2A). This is similar but not identical to that from a previous report, where λ_{max} for this protein was at 351–352 nm.⁴¹ Differences in protein concentration and solvent composition are a likely explanation for the small difference in λ_{max} seen in these two studies. When the protein was excited at 278 nm, where both tyrosine and tryptophan absorb, the maximum of the emission spectrum was at 345 nm. Upon addition of 6 M guanidine HCl, λ_{max} shifted to larger wavelengths by 6 and 4 units for λ_{exc} 278 and 295 nm, respectively (Figure 2A). Furthermore, whereas the intensity of the spectrum at λ_{exc} 295 did not appreciably change upon denaturation, the intensity of the other emission spec-

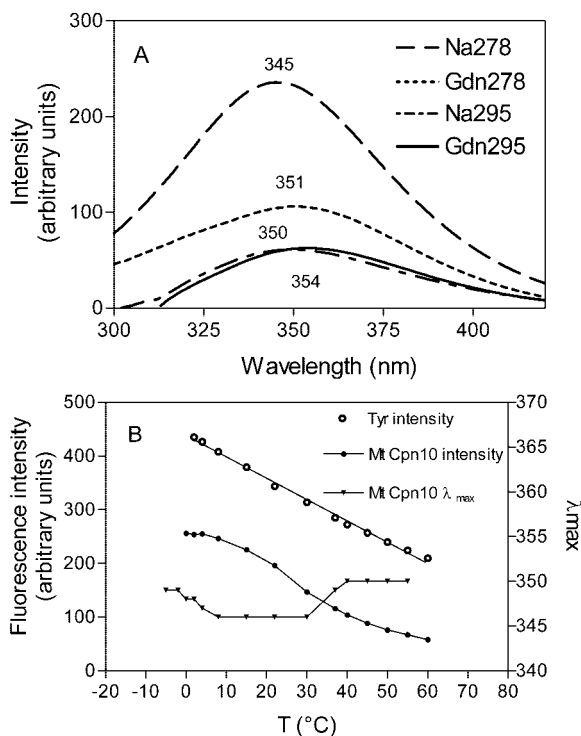


FIGURE 2 (A) Fluorescence emission spectra of monomeric *M. tuberculosis* Cpn10 (0.7 μM) in 2.5 mM PO_4^{3-} , pH 7.4, in its native and denatured (6 M guanidine hydrochloride) forms. The spectra were obtained by excitation at either 295 or 278 nm; T , 22°C. (B) The temperature dependence of λ_{max} and of the intensity of the spectrum of the monomer. As a reference, the spectral variation of a solution containing Tyr at a concentration (2.8 μM) equivalent to that in an *M. tuberculosis* Cpn 10 sample is shown. In this experiment λ_{exc} was set at 278; Na, native; Gdn, guanidine hydrochloride, denatured.

trum dropped by more than half in the presence of guanidine hydrochloride (Figure 2A). These results indicate that in buffer at neutral pH, the protein is partly folded and unfolds completely upon denaturation with guanidinium. Furthermore, Trp50 is largely exposed to solvent in these partially structured monomers, as indicated by the small spectral changes observed upon unfolding.

Figure 2B shows the temperature dependence of the intensity and λ_{max} of the emission spectra obtained by exciting at 278 nm the solution of the monomer and those containing equivalent concentrations of either Tyr or Trp.

The intensity of the spectra of the amino acids varied linearly with changes in temperature, while their respective λ_{max} remained constant (the latter not shown). In contrast, the temperature dependence of the intensity of the spectrum of *M. tuberculosis* Cpn10 exhibited a biphasic behavior characterized by

a steeper variation between approximately 8° and 35°C and two less intense variations below and above these two temperatures. The temperature dependence of λ_{max} exhibited a similar trend, with λ_{max} being constant at 346–347 nm between 4° and 30°C and increasing both below 4°C and above 30°C. These data indicate that at least three different conformational states exist in the temperature range of –5 to +60°C and that those at the two temperature extremes appear to be more disordered, as measured by the red shift in λ_{max} . A further consequence of this experiment is that the monomer must be partially folded at room temperature if unfolding is to take place upon temperature changes.

Circular Dichroism Spectroscopy. The secondary structure composition of monomeric *M. tuberculosis* Cpn10 was investigated by CD spectroscopy. In the first experiment the protein concentration dependence of the secondary structure was monitored in the 13–2.3 μM protein concentration range. Figure 3A shows the changes in molar ellipticities, θ , at 200 and 218 nm and those in λ_{max} observed in 2.5 mM PO_4^{3-} , pH 7.4, at 22°C at the various dilutions of *M. tuberculosis* Cpn10.

At a 13 μM concentration, where self-association takes place (see above), the far-uv CD spectrum of *M. tuberculosis* Cpn10 (Figure 3A) had the same intense negative ellipticity at 203–204 nm and the shoulder at approximately 218 nm seen for the heptamer and used to assign its structure to a mixture of random coil and β -sheet.³³ The negative ellipticity at 203–204 nm progressively shifted to shorter wavelengths upon dilution; at approximately 5 μM it was at 199–200 nm (Figure 3A) and did not change upon further dilution (Figures 3A and 3B), consistent with the analytical ultracentrifugation and size exclusion chromatography conclusions of complete dissociation to monomers below an approximately 4.7 μM protein concentration. The dissociation-induced structural changes are reversible since increasing the concentration of the protein from 0.9 to 9 μM restored the negative maximum at 202–203 nm and induced self-association (data not shown).

CD spectra with a negative ellipticity at or below 200 nm are generally attributed to the unordered conformation. Therefore, it would appear from the CD data that the subunits of the various oligomeric forms of *M. tuberculosis* Cpn10 become unordered upon dissociation. On the other hand, the molar ellipticity at about 218 nm remained constant throughout the entire dilution study, indicating the presence of secondary structure elements even at the lowest concentration of protein measured, namely, 2.3 μM (Figures 3A and

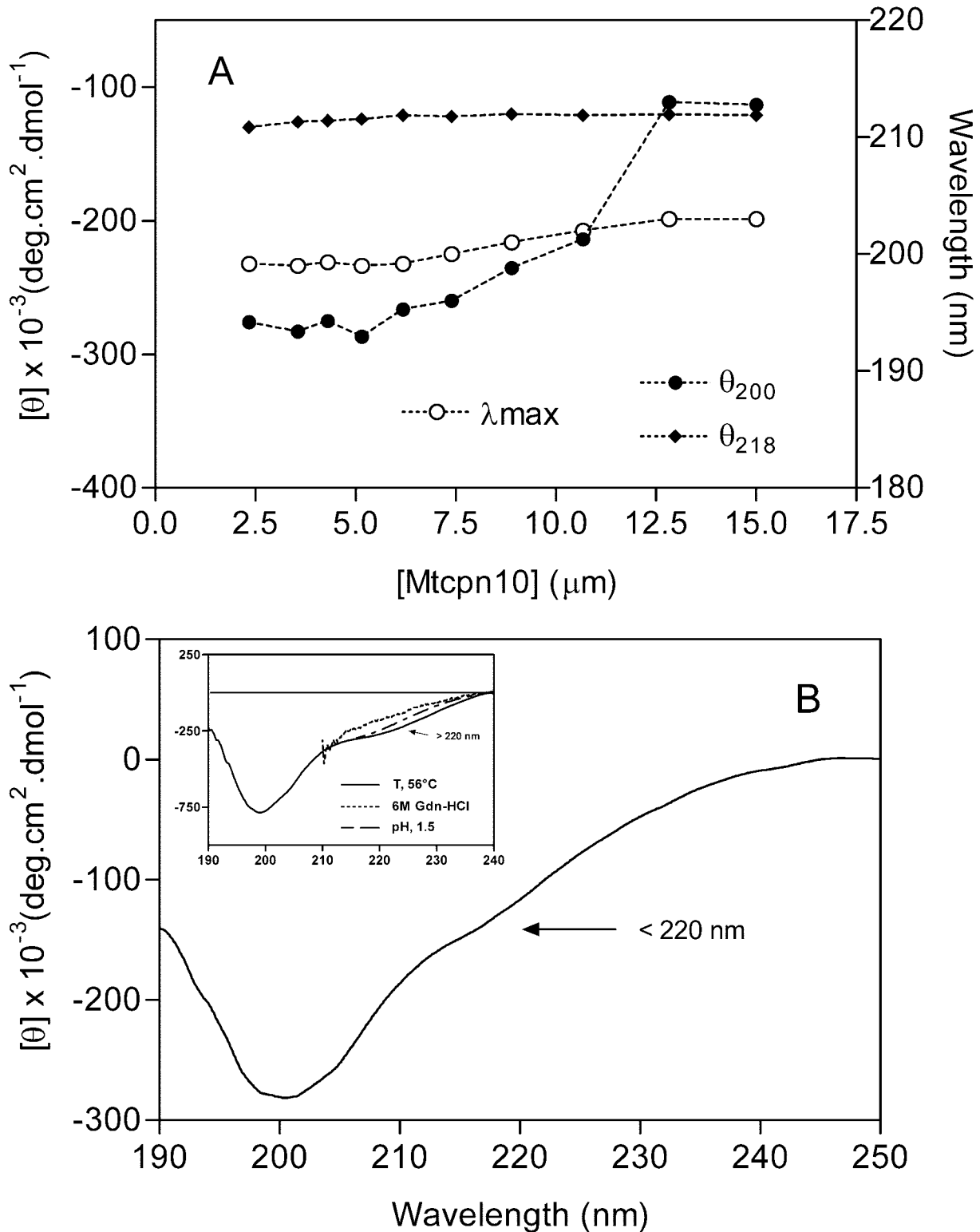


FIGURE 3 (A) The concentration dependence of λ_{max} and of the molar ellipticities at 200 and 218 nm of the CD spectra of *M. tuberculosis* Cpn10 in 2.5 mM PO_4^{3-} , pH 7.4, are shown at a 13–2.3 μM protein concentration range; T , 22°C. (B) The far-ultraviolet CD spectrum of monomeric *M. tuberculosis* Cpn10 (2.3 μM) in 2.5 mM PO_4^{3-} , pH 7.4. (Inset) Far-ultraviolet CD spectra of monomeric *M. tuberculosis* Cpn10 in 2.5 mM PO_4^{3-} , pH 7.4, 56°C; 2.5 mM PO_4^{3-} , pH 1.5, 25°C; 2.5 mM PO_4^{3-} , pH 7.4, plus 6 M guanidine hydrochloride.

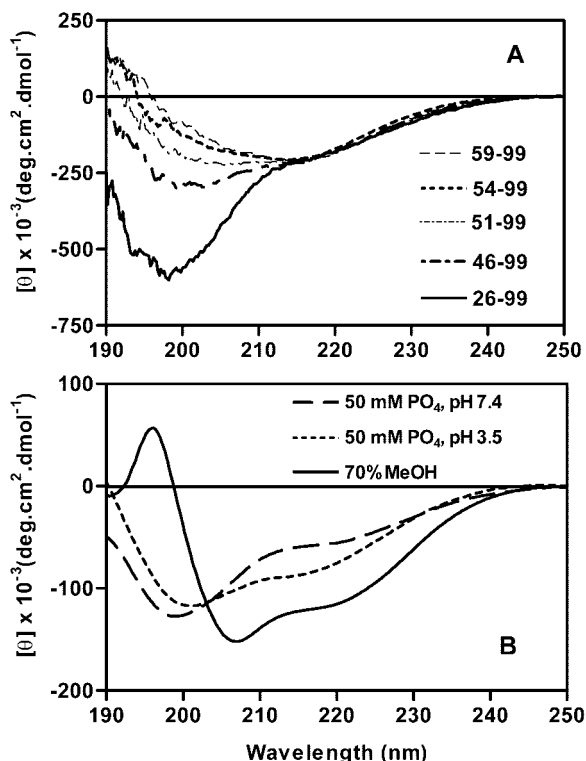


FIGURE 4 Far-ultraviolet CD spectra of *M. tuberculosis* Cpn10 N-terminally shorter synthetic fragments. (A) Peptides 26-99, 46-99, 51-99, 54-99, and 59-99 (10 $\mu\text{g}/\text{mL}$ each) in 2.5 mM PO_4^{3-} , pH 7.4. The order in which the spectra appear in the figure follows their length, i.e., the spectrum of 26-99 is the most intense at about 199–200 nm and that of peptide 59-99 is the least intense in this region. (B) Peptide 75-99 in 2.5 mM PO_4^{3-} , pH 7.4 and 3.5, and in 7.5 mM $\text{PO}_4^{3-}/\text{MeOH}$ (30:70, v/v).

3B). This conclusion was confirmed by the decrease in signal intensity in the secondary structure region of the spectrum upon addition of 6 M guanidine hydrochloride (Figure 3B, inset).

Collectively these data confirmed the above conclusions of the existence of partially folded monomers in dilute solutions of protein.

N-Terminally Shorter Peptides

To identify regions that may be structured in the partially folded monomer, the synthetic peptides 26-99, 46-99, 51-99, 54-99, 59-99, 65-99, and 75-99 were studied in dilute solutions and neutral pH, where they are known to be monomeric.³³ The CD spectra of these polypeptides in 2.5 mM PO_4^{3-} , pH 7.4, are shown in Figure 4. A clear reduction in the ellipticity at 199 nm is observed as the chain length decreases from peptide 26-99 to peptide 59-99. In contrast the

intensity of the ellipticity at 218 nm remains constant in these sequences and peptides 54-99 and 59-99 show the typical antiparallel β -sheet profile, with a negative maximum at 218 nm. There is very little or no random coil at all in these peptides, as indicated by the absence of a well-defined band at 199 nm. Further shortening of the chain, as in peptide 65-99, reversed this trend and the unordered conformation increases again (not shown). It would appear, therefore, that one or more β -sheets are contained in the C-terminal half of the partially folded monomer. In contrast, the N-terminal region appears to be largely disordered in these monomers. One notable exception to this general trend is represented by peptide 75-99, whose CD spectrum at neutral pH contains the negative maximum at 199 nm and a well-defined negative ellipticity at around 222 nm, the latter typical of the α -helix (Figure 4B). At acidic pH, or in the presence of methanol, the negative ellipticity at 222 nm increased, while the other negative maximum red-shifted to 201 and 206 nm, respectively (Figure 4B). Thus, this peptide is able to adopt a partially helical conformation whose stability increases at acidic pH or in the presence of organic solvents. It is therefore possible that, in addition to conformations dominated by the β -sheet and random-coil structures, the *M. tuberculosis* Cpn10 monomer might form partially helical conformers.

Perturbation of the Conformational Equilibrium of the *M. tuberculosis* Cpn10 Monomer

From the results so far described it is reasonable to conclude that the solution structure of the monomer is best described as being composed of completely unfolded conformers and partially folded conformers in equilibrium with each other. Conformational equilibria such as this can be perturbed by changes in the solvent composition or solution conditions and this often leads to the preferential accumulation of one or more conformers. We therefore analyzed dilute solutions of *M. tuberculosis* Cpn10 under different conditions of pH, temperature, and solvent composition.

The pH Study. In the first experiment, the effect of the solution pH on the monomer was studied in the pH interval 7.4–1.9. The results are shown in Figure 5. Below pH 7.4, the ellipticity at 200 nm decreased and shifted to longer wavelengths. Between pH 5.8 and 2.9, the spectra were essentially superimposable and similar to those of oligomeric *M. tuberculosis* Cpn10,^{30,31,33} having a negative maximum at approximately 204 nm and a broad band in the secondary

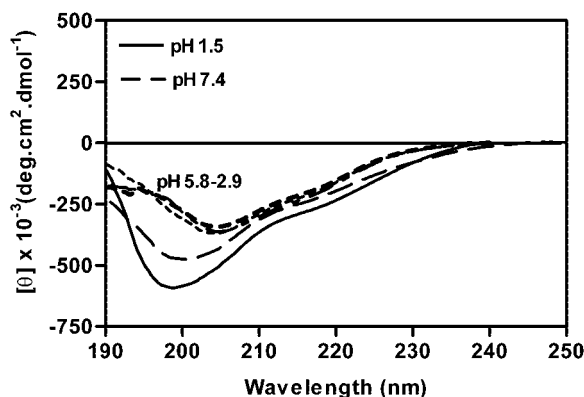


FIGURE 5 Far-ultraviolet CD spectra of a dilute solution of *M. tuberculosis* Cpn10 ($2.3 \mu\text{M}$) in 2.5 mM PO_4^{3-} showing the pH dependence of the protein structure in the pH range 7.4–1.5. The three spectra in the pH range 5.8–2.9 are essentially superimposable and are not individually labeled.

structure region (Figure 5). At pH 1.5, the main ellipticity returned to 199–200 nm, suggesting the occurrence of acid-induced denaturation (Figure 5). Notice, however, that the CD spectrum at this pH contains a small but significant amount of secondary structure which is skewed toward the helical region ($> 220 \text{ nm}$) (Figure 5).

The shape of the spectra in the pH interval 5.8–2.9 suggests that the monomer self-associates under these conditions. To verify this conclusion, a pH 3.5 solution containing approximately $0.9 \mu\text{M}$ *M. tuberculosis* Cpn10 was subjected to sedimentation velocity and equilibrium studies. Higher molecular weight species were thus detected that have sedimentation Svedberg coefficients of 1.2, 2.3, and 3.2 and are present in proportions of 58, 37, and 5%, respectively. By sedimentation equilibrium the average M_r of the protein was calculated to be 18.3 kDa, which is consistent with the presence of oligomeric species at this pH.

Thus the monomer self-associates in the pH range 2.9–5.8 and has a secondary structure composition (β -sheet and random coil) similar to that observed for oligomeric *M. tuberculosis* Cpn10 at neutral pH.³³

Temperature Study. In the second study, the temperature dependence of the secondary structure of the monomer ($1.4 \mu\text{M}$) was investigated in the temperature range -7°C to 56°C . The corresponding CD spectra are shown in Figures 6A and 6B, while the temperature dependence of θ at 199 and 222 nm is shown in Figure 7A. All spectral changes were fully reversible (not shown).

The spectrum of the monomer in 2.5 mM PO_4^{3-} , pH 7.5, did not change when the temperature was varied between 14° and 24°C and contained the same

negative ellipticity at 200 nm and the shoulder at 218 nm seen at the end of the protein concentration study of Figure 3B. However, as the temperature decreased below 14°C , a progressive increase in the random coil ellipticity at 199–200 nm occurred, which was paralleled by a decrease in the secondary structure at 218 nm (Figure 6A). These spectral changes were associated with an isodichroic point at approximately 208 nm (Figure 6A), indicating the occurrence of a two-component equilibrium. One component is the conformation(s) present in the temperature interval 14 – 24°C , and the other component is the cold-denatured monomer the complete formation of which was not possible to observe due to freezing of the solution below -7°C .

When the temperature of the solution was raised above 24°C , additional variations occurred in the monomer which were also characterized by an increase in the random coil structure at 199 nm. However, unlike in protein below 14°C , the secondary structure of the monomer increased upon heating and

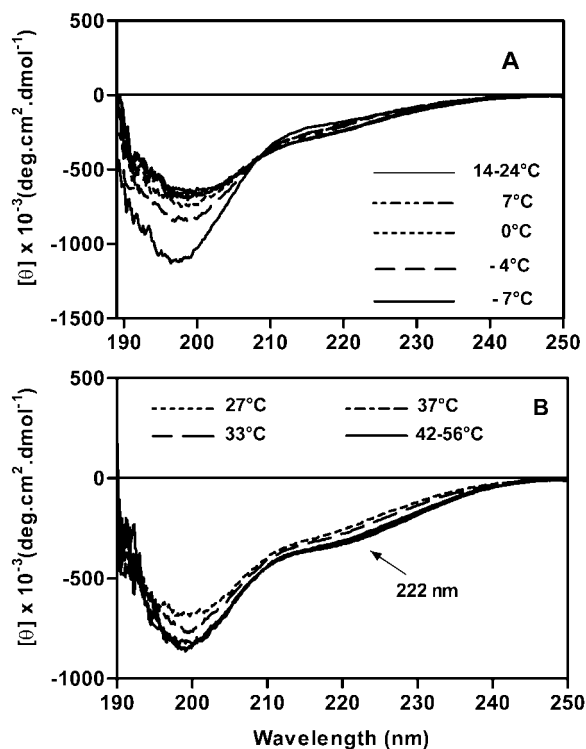


FIGURE 6 Temperature dependence of the CD spectra of monomeric *M. tuberculosis* Cpn10 ($2.3 \mu\text{M}$) in 2.5 mM PO_4^{3-} , pH 7.4. (A) Temperature interval, -7°C to $+24^\circ\text{C}$. The intensity of the negative maximum below 200 nm decreases as the temperature increases from -7°C to $+24^\circ\text{C}$. (B) Temperature interval, $+27^\circ\text{C}$ to $+56^\circ\text{C}$. The intensity of the negative maximum below 200 nm increases as the temperature increases from $+27^\circ\text{C}$ to $+56^\circ\text{C}$.

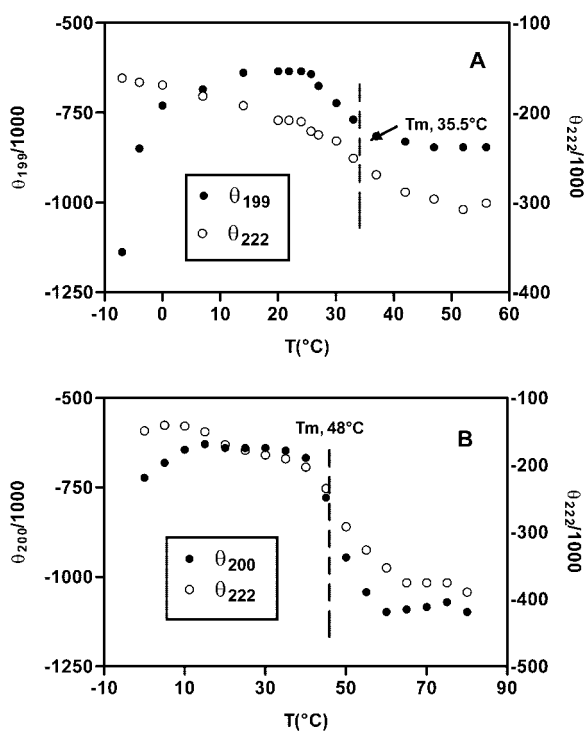


FIGURE 7 Temperature dependence of the molar ellipticities (θ) at 199/200 and 222 nm of monomeric (A) and heptameric (B) *M. tuberculosis* Cpn10. The CD spectra of the monomer were acquired in 50 mM PO_4^{3-} , pH 7.4, at a 2.3 μM total protein concentration. The solution of the Cpn10 heptamer contained about a 30 μM protein concentration in 100 mM PO_4^{3-} , pH 7.4, plus 2.5 mM MgCl_2 .

the shoulder at 218 nm in the spectrum at room temperature shifted to 222 nm at 45°C (Figure 7B). No further changes were observed upon further heating up to 56°C. The melting temperature (T_m) of this transition is about 35.5°C (Figure 7A).

It is known that Cpn10 heptamers dissociate to monomers at high temperature.^{28,30,31} Therefore, to verify whether thermal dissociation of oligomeric *M. tuberculosis* Cpn10 induces the same CD variations observed with the monomer, spectra of heptameric Cpn10 were recorded at different temperatures. The results are shown in Figure 7B. As can be seen, Θ_{222} increased with temperature and was maximal at approximately 65°C. Above this temperature the spectra were essentially identical (not shown). The T_m of this transition is approximately 48°C and larger therefore than that of the 35.5°C seen for the monomer (Figure 7B). Interestingly, as with the isolated monomer, cold-denaturation occurs in the heptamer below a temperature of approximately 15°C³³ (Figure 7B).

In conclusion, the partially folded monomers detected at room temperature completely unfold at low temperature, while at higher temperatures a confor-

mation remains which is largely unfolded but has some residues in the α -helical structure. This conformation is independent of the origin of the monomer, i.e., from dilution-induced dissociation or thermally induced dissociation of oligomeric Cpn10.

These results are fully in agreement with those obtained by fluorescence spectroscopy where cold- and thermal-denaturation were seen below 4–8°C and above 30–35°C, respectively.

Mixed Solvents. The temperature and pH studies together with the CD spectra of peptide 75-99 (Figure 4B) suggest that the solution conformational equilibrium of the monomer may contain small amounts of a partially helical conformation(s) and that this conformation has a C-carboxyl α -helix. The existence of a stable partially helical monomer has been shown in organic solvent/buffer mixtures or in the presence of detergents¹⁸ (Figure 8A). This monomer contains an amphiphilic α -helix (residues 1–16) and is in equilibrium with a dimer having an all- β structure and predominating at higher concentrations (> 18 μM) or at low temperature (Figure 8A).¹⁸

Here, we further analyzed the structure of the partially helical monomer and recorded the CD spectra of the protein's N-terminally shorter fragments (approximately 10 $\mu\text{g}/\text{mL}$ each) in 70% MeOH. In Figure 8B, the intensity at 222 nm, which was used as an approximate measure of the helical content in the polypeptide chain, is plotted against the polypeptide length. There is a drop in α -helicity on going from the whole sequence to peptide 26-99 and from peptide 75-99 to peptide 91-99 (Figure 8B); in contrast, the helical content is practically constant in the other peptides (Figure 8B). These results are consistent with the N-terminal α -helix identified in the other study¹⁸ and confirm that a second helix is present at the C-terminus of the partially helical monomer. There appear to be no other helical regions in the partially helical monomer from these data.

DISCUSSION

The x-ray structure of Cpn10 heptamers resembles a dome with an oculus in its roof.^{8–11,42} At the bottom edge of the dome there are seven loops, the so-called mobile loops (residues 17–35),⁴³ which interact with Cpn60 and, in the case of *M. tuberculosis* Cpn10, with the mobile loops of a neighboring Cpn10 heptamer.⁷ In the middle of the subunit there is another loop (the “roof loop”), from residue 51 to residue 56, which forms the roof of the heptamer dome. The oculus of the dome is lined by a ring of negative carboxylates.

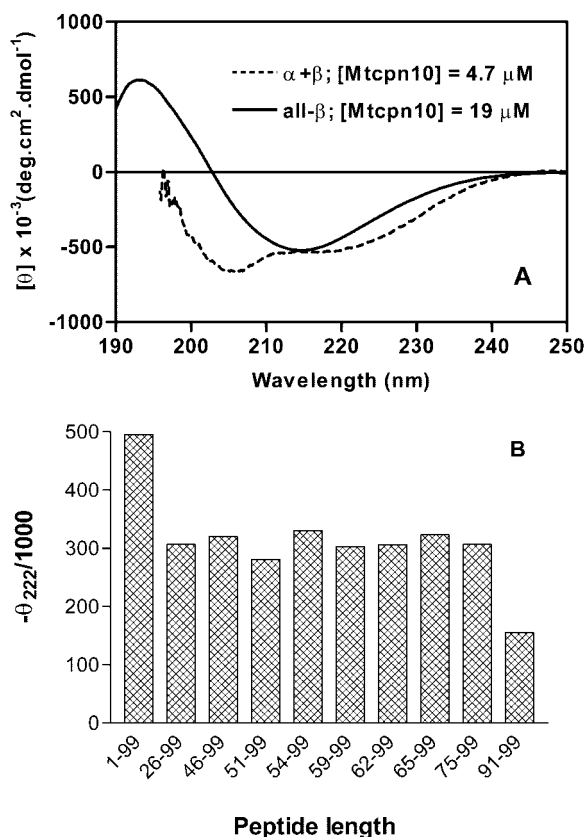


FIGURE 8 (A) Far-ultraviolet CD spectra of *M. tuberculosis* Cpn10 in 100 mM PO_4^{3-} /MeOH (1:1, v/v) at 4.7 and 19 μM concentrations. The increase in concentration causes the protein to change from partially helical to all- β and this is due to its dimerization.¹⁸ The spectrum of the protein at the lower concentration starts from 196 nm due to a high level of noise below this wavelength. (B) The molar ellipticity (θ) at 222 nm as measured in the protein's N-terminally shorter synthetic peptides (approximately 10 $\mu\text{g}/\text{mL}$ each) in 155 mM PO_4^{3-} /MeOH (3:7) mixtures.

In *M. tuberculosis* Cpn10 they are provided by Asp51, Glu52, Asp53, and Glu55 of each subunit and in *E. coli* Cpn10 by Glu52 and Glu55 only. The accumulation of acidic residues generates significant coulombic repulsion between the roof loops, resulting therefore in an increased flexibility of the dome and instability of the heptameric structure.^{8,12,42} Consistent with this observation is the increased stability of heptameric Cpn10s observed in the presence of divalent metal cations or at low pH.^{31,33,41} Under these conditions, the negative charges of the roof carboxylates are thought to be neutralized by divalent ions or by protons.^{7,33,41}

The core domain of each subunit is a β -barrel made of two orthogonal antiparallel β -sheets. The strongest inter-subunit interactions occur across the

first (β 1, 4–7) and last (β 7, 93–98) β -strands of neighboring subunits. This association is compounded by the hydrophobic interfaces of adjacent subunits and is the main driving force in the formation of *E. coli* Cpn10 heptamers from monomers.³¹ The total nonpolar surface accessible to solvent in the structure of each isolated subunit is much larger than that typically found for globular proteins with a similar number of residues.³¹ This unusually large hydrophobic surface becomes available to solvents upon dissociation and conformational changes are therefore likely to occur in the isolated monomer. Thermodynamic studies have suggested that monomers arising from the dissociation of the *E. coli* Cpn10 heptamer are largely unfolded at room temperature.³¹ On the other hand, in urea- or guanidinium-induced denaturation experiments, partially folded monomers of *E. coli* Cpn10 and human Cpn10 have been identified which are only marginally stable at room temperature.^{28,32,35}

In this work we identified the conditions which favor dissociation of oligomeric *M. tuberculosis* Cpn10 to monomers and studied the solution structure of the latter in the absence of denaturants. We found that at neutral pH and in the absence of divalent cations, the protein reversibly dissociates to monomers below an approximately 4.7 μM concentration. This is significantly larger than the approximately 0.1 μM concentration found for the *E. coli* Cpn10 heptamer both in the absence and in the presence of divalent cations^{29,30} (and P. Mascagni, manuscript in preparation) and indicates a decreased stability of oligomeric *M. tuberculosis* Cpn10 compared to the *E. coli* homologue. The reasons for this difference likely include the larger number of opposing negative charges lining the orifice dome of the *M. tuberculosis* Cpn10 heptamer compared with the *E. coli* Cpn10 (see above). The increased ability of the *M. tuberculosis* Cpn10 monomer to self-associate observed at acidic pH (Figure 5), where neutralization of the exposed carboxylates occurs, adds further support to this conclusion.

At neutral pH, the *M. tuberculosis* Cpn10 monomer forms partially folded structures. Evidence for this conclusion includes (i) the frictional fraction ratio of about 1.4 and the axial ratio of the equivalent prolate ellipsoid of about 5, indicating that the structure of the monomer is not completely unfolded and elongated in shape, (ii) the small but significant ellipticity found in the region 215–225 nm of the CD spectrum of the monomer, suggesting the existence of secondary structure (Figure 3); (iii) the guanidinium-induced changes in the fluorescence emission spectra of the monomer (Figures 2A and 2B), which also

imply the presence of folded structures at room temperature; (iv) the partial or complete denaturation occurring under various conditions (Figures 2, 3, 5–7), which again implies the existence of secondary structure elements; and by analogy (v) reports that other monomeric Cpn10s form partially stable structures at room temperature.^{28,32,35}

The existence of structured regions in the monomer was also inferred from the CD spectra of the N-shorter forms of *M. tuberculosis* Cpn10 (Figure 4A), which indicated that secondary structure, predominantly β -sheet, might be present in the C-terminal half of the protein. In particular a stable β -sheet(s) was assigned to the region C-carboxyl to Pro59 based on the combined CD data on the N-shorter forms (Figure 4A) and the fluorescence emission spectra of the protein (Figure 2A). In contrast, the N-terminal region is disordered in these monomers, as indicated not only by the CD spectra of the larger N-terminally shorter peptides (e.g., peptides 26–99 and 46–99, Figure 4A) but also by our previous observation of a mainly random coil structure for the C-terminally shorter peptide 1–58, as determined by CD spectroscopy.³³

The disordered N-terminal half of this conformation contains one of the two sequences (peptide 26–35) of the *M. tuberculosis* Cpn10 monomer that were identified as being active in bone resorption.²⁶ This sequence occurs in the mobile loop region, (peptide 17–35) which is also disordered in the heptamer but acquires the structure of a β -hairpin when bound to Cpn60 in the Cpn10–Cpn60 protein-folding complex.⁴ It is possible therefore that the mechanism of bone resorption is mediated by the same unordered to β -hairpin structural transition.⁴³ Consistent with this conclusion is the identification of Cpn60s on the cell surface⁴⁴ which could therefore act as receptors for *M. tuberculosis* Cpn10 in the bone resorption assay.

The conformation with a structured C-terminal half has general characteristics that resemble those of the heptamer subunits where the N-terminal half is more disordered and the C-terminal half contains four β -strands, namely, β 4, 66–71; β 5, 76–80; β 6, 83–90; and β 7, 93–98.⁷ However, the formation of β -sheets in the C-terminal half of the heptamer depends to a large degree on interactions with β -sheets in the N-terminal half of a neighboring subunit. If these are absent, then the β -sheet topology in the monomer would have to be reoriented. One possible rearrangement of the C-terminal β -strands has been proposed previously based on sequence homology with HLA antigens.⁴⁵

The conformation with a C-terminal β -sheet(s) is stable in a very narrow range of temperature, between 14° and 24°C; below 14°C denaturation occurs. This

is unusual because the observation of cold-denaturation at these relatively high temperatures is rare for proteins in the absence of denaturants or at low pH. Reasons for this difference may include the mechanism of cold-denaturation and the heat-shock nature of molecular chaperones such as *M. tuberculosis* Cpn10. Thus, on the one hand, cold-denaturation is believed to be caused by the interactions between water and the nonpolar groups that become available upon protein unfolding,^{46,47} and on the other hand, nonpolar groups are more abundant in molecular chaperones than in monomeric globular proteins having similar molecular weight.⁴⁸ For instance, in *M. tuberculosis* Cpn10, the frequency of branched nonpolar residues such as Val, Leu, and Ile is approximately 5% larger than that found in globular proteins and this difference increases to approximately 7% in the more structured C-terminal region (i.e., 59–99) of the monomer. An increased concentration in nonpolar residues is typical of warm-adapted enzymes, as the hydrophobic effect becomes stronger with increasing temperature and this confers increased stability on the active conformation of the enzyme⁴⁹ (see also references therein). The same therefore may be true for molecular chaperones, which have evolved to maintain their chaperoning activity at above physiological temperatures.

Therefore, the early cold-denaturation of the *M. tuberculosis* Cpn10 monomer may just be a consequence of its increased concentration in hydrophobic residues and of the increased number of water/nonpolar residue interactions that occur upon unfolding.

Above 24°C, the monomer undergoes a second unfolding step which, however, does not lead to complete denaturation. The T_m of this transition (about 35.5°C) and that associated with the thermal dissociation of heptameric *M. tuberculosis* Cpn10 (48°C) are considerably smaller than the values of 70–76°C and 68–72°C found for *E. coli* Cpn10 and human Cpn10, respectively,^{28,31} again suggesting a decreased stability of oligomeric *M. tuberculosis* Cpn10 compared to the other Cpn10s.

At high temperature or under strong acidic conditions, the *M. tuberculosis* Cpn10 monomer is not completely denatured and contains residues in the α -helical structure (Figure 3B, inset). A similar situation also exists for monomeric *E. coli* Cpn10, where an increase in molar ellipticity at 222 nm is clearly seen during the thermal dissociation of the heptamer to a monomer³¹ (also see Figure 3 in Boudker et al.³¹). Although there are no α -helices in the X-ray structures of *E. coli* or *M. tuberculosis* Cpn10 heptamers, their existence in Cpn10s has been predicted based on sequence and the α -helical structure assigned to pep-

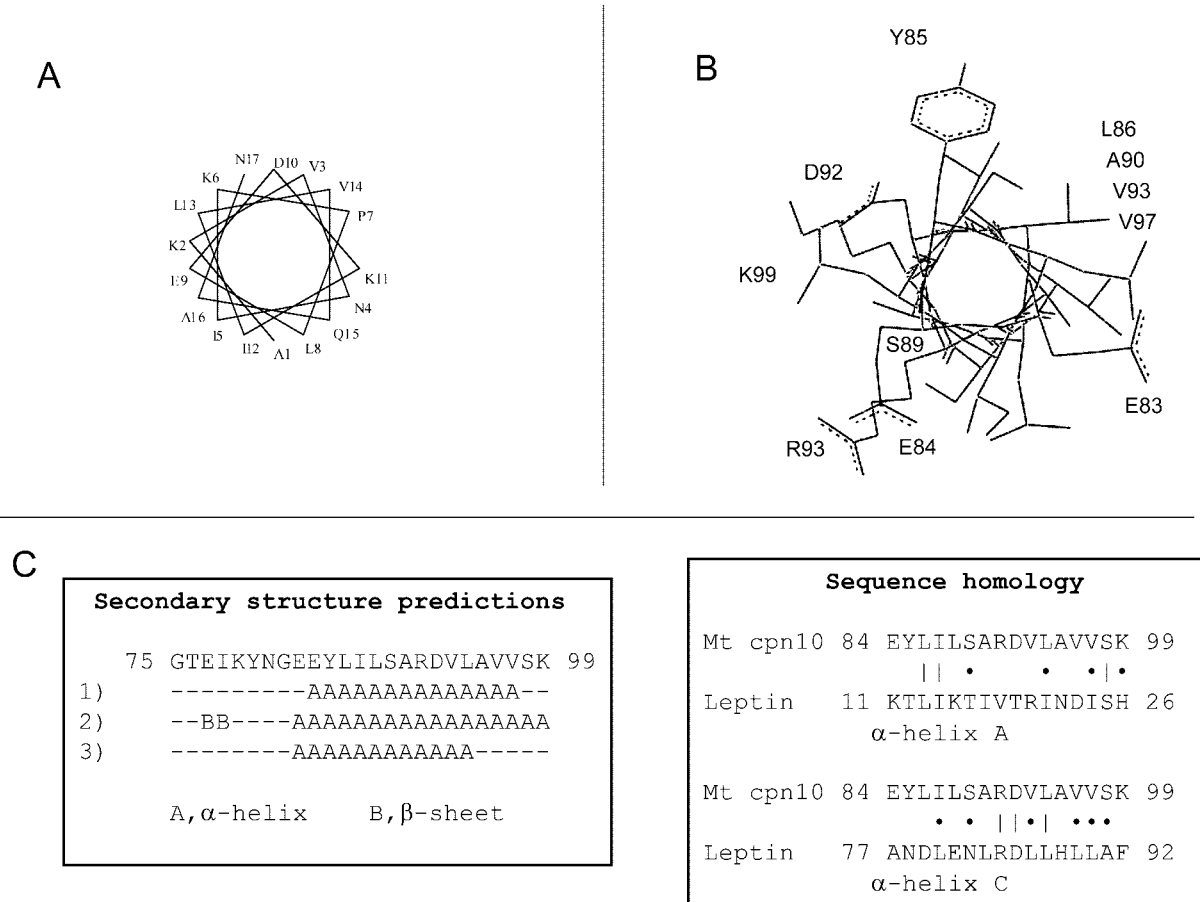


FIGURE 9 (A) The amphiphilic α -helical structure of peptide 1-25 found in solution.¹⁸ (B) Model of the amphiphilic α -helix predicted for sequence 84-99 and viewed along the helical axis toward the N-terminus. (C) Secondary structure prediction for the sequence 75-99 of *M. tuberculosis* Cpn10 and its sequence homology to leptin. The algorithms of Qian and Sejdenovski,⁵³ Garnier et al.,⁵⁴ and Maxfield and Scheraga⁵⁵ were used within the Sybyl program (Tripos Associates, Inc.) for secondary structure prediction.

tides 2-13, 27-38, and 83-99.³³ Furthermore, an α -helix encompassing a sequence that corresponds to 31-35 in *M. tuberculosis* Cpn10 exists in the crystal structure of bacteriophage T4 co-chaperonin Gp31.⁹ Additional evidence for the propensity of the *M. tuberculosis* Cpn10 monomer to form α -helical structures is provided by our previous study of the monomer in mixed solvents or in the presence of detergent micelles. Under these conditions, which are believed to mimic the biological membrane, the monomer consistently forms a stable partially helical conformation.¹⁸ This conformation contains an N-terminal amphiphilic helix (sequence 1-16, Figure 9A) that selectively associates with negatively charged micelles. This and other observations led us to propose a correlation between the ability of the monomer to form helical structures and the secretion of *M. tuberculosis* Cpn10 outside the bacillus.¹⁸ An additional

helix may be present at the carboxyl end of the partially helical monomer, as suggested by the CD spectra of the synthetic peptide 75-99. Furthermore, secondary structure predictions³³ (Figure 9C) indicate that from residue 83 to residue 99, the peptide is likely to be α -helical and mostly amphiphilic (Figure 9B). This helix has significant homology with the amphiphilic α -helices A (44%) and C (56%) on the receptor-binding site of the cytokine leptin^{4,50} (Figure 9C). Since leptin, a 16-kDa cytokine, is able to stimulate monocyte IL-6 synthesis,⁵¹ the ability of monomeric *M. tuberculosis* Cpn10 and of peptide 75-99 to induce the synthesis of this cytokine may be due to leptin receptor activation (B. Henderson, unpublished observation).

Interestingly, in the heptamer the C-terminal region contains one β -strand ($\beta 7$) forming an antiparallel β -sheet with the N-terminal β -strand ($\beta 1$) of a

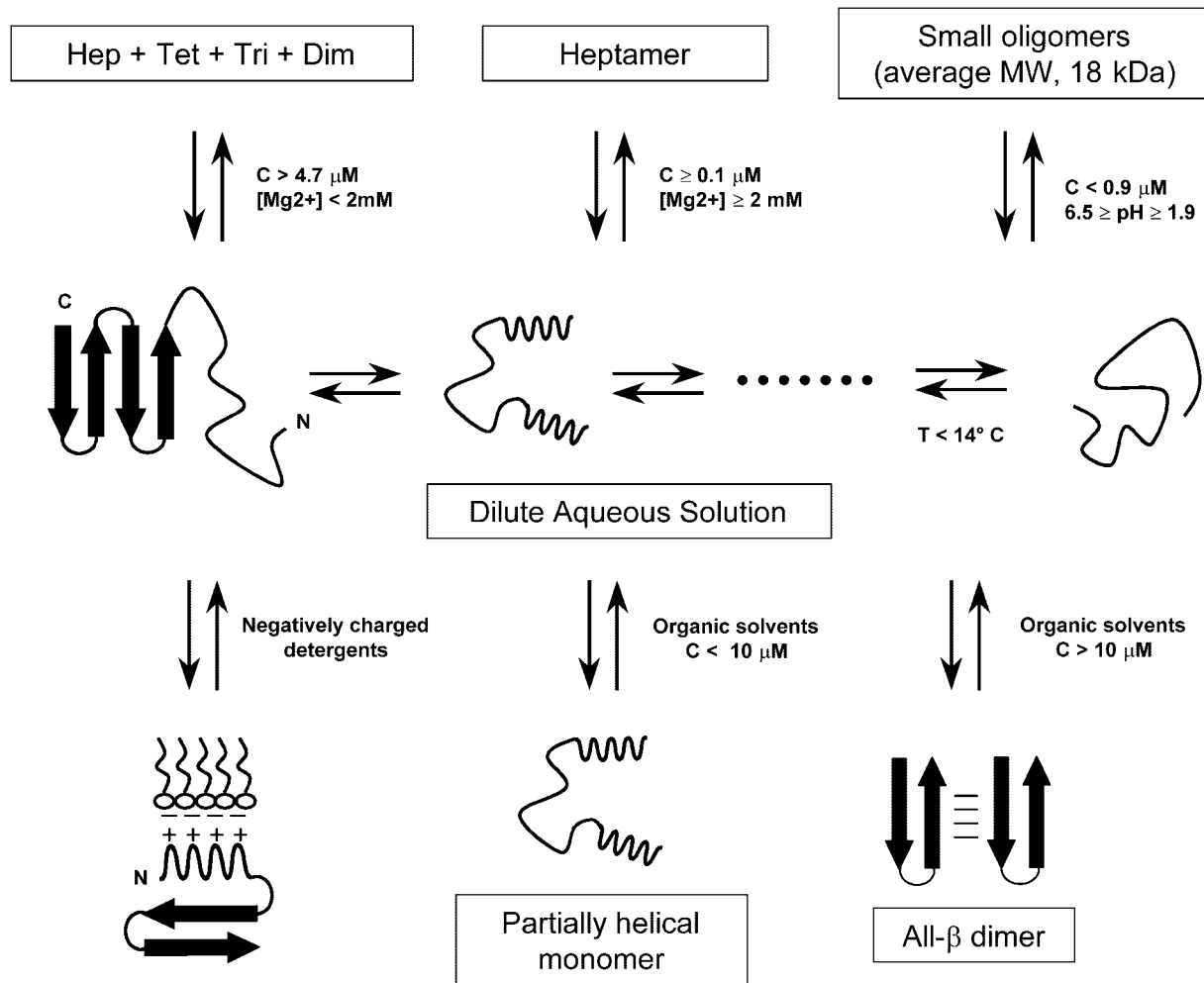


FIGURE 10 Scheme illustrating the equilibria involving the various structures of *M. tuberculosis* Cpn10 identified in this and in related studies^{33,18} (see also P. Mascagni, manuscript in preparation).

neighboring subunit. Thus, both the N- and the C-termini of *M. tuberculosis* Cpn10 contain the protein's association motifs and are able to form two distinct structures, the β -strand in the oligomer and the α -helix in the partially helical monomer.

There was no evidence for the existence of the third predicted α -helix of sequence 27–38.

The partially helical structure may be important not only in the mechanism of transport of the protein outside the bacillus or in the synthesis of IL-6 (B. Henderson et al., unpublished), it may also be involved in the other biological activities of the monomer (e.g., bone resorption²⁶) since they are measured at 37°C, where the transition from partially β monomer to partially α -helical monomer has already occurred (Figure 6B).

In conclusion, we have shown that in dilute solutions and at neutral pH, *M. tuberculosis* Cpn10 is completely dissociated into monomers and that these

monomers undergo structural changes in response to changes in environmental conditions such as solvent composition, pH, and temperature. Reassociation of monomers to oligomers is favored at acidic pH and by an increase in protein concentration. Interestingly, oligomers other than the heptamer are generated under both these conditions. In Figure 10 a scheme summarizing the structural equilibria involving *M. tuberculosis* Cpn10 is shown.

An attempt was made to correlate the structural findings with the diverse biological activities of the *M. tuberculosis* Cpn10 monomer. In this respect, the response of the monomer to pH may be more interesting in terms of the function of *M. tuberculosis* Cpn10 as a cell signaling protein.⁵² Ingestion of *M. tuberculosis* by macrophages results in the bacterium entering endosomes in which the pH may be reduced by several units. It is known that *M. tuberculosis* Cpn10 is released in this environment,¹⁸ al-

though the mechanism of survival is not known. This study suggests that the ability of the monomer either to adopt partially helical structures or to associate to small oligomers at low pH or both may contribute to protein survival in the endosome.

REFERENCES

- Hartl, F. U.; Hayer-Hartl, M. *Science* 2002, 295, 1852–1858.
- Sigler, P. B.; Xu, Z.; Rye, H. S.; Burston, S. G.; Fenton, W. A.; Horwich, A. L. *Annu Rev Biochem* 1998, 67, 581–608.
- Gottesman, M. E.; Hendrickson, W. A. *Curr Opin Microbiol* 2000, 3, 197–202.
- Xu, Z.; Horwich, A. L.; Sigler, P. B. *Nature* 1997, 388, 741–750.
- Boisvert, D. C.; Wang, J.; Otwinowski, Z.; Horwich, A. L.; Sigler, P. B. *Nat Struct Biol* 1996, 3, 170–177.
- Braig, K.; Otwinowski, Z.; Hegde, R.; Boisvert, D. C.; Joachimiak, A.; Horwich, A. L.; Sigler, P. B. *Nature* 1994, 371, 578–586.
- Roberts, M. M.; Coker, A. R.; Fossati, G.; Mascagni, P.; Coates, A. R. M.; Wood, S. P. *J Bacteriol* 2003, 185, 4172–4185.
- Hunt, J. F.; Weaver, A. J.; Landry, S. J.; Gierasch, L.; Deisenhofer, J. *Nature* 1996, 379, 37–45.
- Hunt, J. F.; van der Vies, S. M.; Henry, L.; Deisenhofer, J. *Cell* 1997, 90, 361–371.
- Roberts, M. M.; Coker, A. R.; Fossati, G.; Mascagni, P.; Coates, A. R.; Wood, S. P. *Acta Crystallogr D* 1999, 55, 910–914.
- Taneja, B.; Mande, S. C. *Curr Science* 2001, 81, 87–91.
- Taneja B.; Mande, S. C. *Protein Eng* 1999, 12, 815–818.
- Fattorini, L.; Creati, R.; Nisini, R.; Pietrobono, R.; Fan, Y.; Stringaro, A.; Arancia, G.; Serilupi-Crescenzi, O.; Iona, E.; Orefici, G. *J Med Microbiol* 2002, 51, 1071–1079.
- Wu, Y. L.; Lee, L. H.; Rollins, D. M.; Ching, W. M. *Infect Immun* 1994, 62, 4256–4260.
- Ryan, M. T.; Hoogenraad, N. J.; Hoj, P. B. *FEBS Lett* 1994, 337, 152–156.
- Vanet, A.; Labigne, A. *Infect Immun* 1998, 66, 1023–1027.
- Sadacharan, S. K.; Cavanagh, A. C.; Gupta, R. S. *Histochem Cell Biol* 2001, 116, 507–517.
- Fossati, G.; Izzo, G.; Rizzi, E.; Gancia, E.; Modena, D.; Moras, M. L.; Niccolai, N.; Giannozzi, E.; Spiga, O.; Bono, L.; Marone, P.; Leone, E.; Mangili, F.; Harding, S.; Errington, N.; Walters, C.; Henderson, B.; Roberts, M. M.; Coates, A. R. M.; Casetta, B.; Mascagni, P. *J Bacteriol* 2003, 185, 4256–4267.
- Henderson, B.; Nair, S. P.; Coates, A. R. *Inflamm Res* 1996, 1, 155–158.
- Alder, G. M.; Austen, B. M.; Bashford, C. L.; Mehlert, A.; Pasternak, C. A. *Biosci Rep* 1990, 10, 509–518.
- Friedland, J. S.; Shattock, R. J.; Johnson, J. D.; Remick, D. G.; Holliman, R. E.; Griffin, G. E. *Clin Exp Immunol* 1993, 91, 282–286.
- Retzlaff, C.; Yamamoto, Y.; Hoffman, P. S.; Friedman, H.; Klein, T. W. *Infect Immun* 1994, 62, 5689–5693.
- Verdegaal, M. E.; Zegveld, S. T.; van Furth, R. J. *Immunol* 1996, 157, 369–376.
- Cavanagh, A. C.; Morton, H. *Eur J Biochem* 1994, 222, 551–560.
- Kirby, A. C.; Meghji, S.; Nair, S. P.; White, P.; Reddi, K.; Nishihara, T.; Nakashima, K.; Willis, A. C.; Sim, R.; Wilson, M. and Henderson, B. *J Clin Invest* 1995, 96, 1185–1194.
- Meghji, S.; White, P. A.; Nair, S. P.; Reddi, K.; Heron, K.; Henderson, B.; Zaliani, A.; Fossati, G.; Mascagni, P.; Hunt, J. F.; Roberts, M. M.; Coates, A. R. M. *J Exp Med* 1997, 186, 1241–1246.
- Coates, A. R. M. *The Chaperonins*; Ellis, J. R., Ed.; Academic Press: London, 1996; pp. 267–296.
- Guidry, J. J.; Moczygemba, C. K.; Steede, N. K.; Landry, S. J.; Wittung-Stafshede, P. *Protein Sci* 2000, 11, 2109–2117.
- Zondlo, J.; Fisher, K. E.; Lin, Z.; Ducote, K. R.; Eisenstein, E. *Biochemistry* 1995, 34, 10334–10339.
- Seale, J. W.; Gorovits, B. M.; Ybarra, J.; Horowitz, P. M. *Biochemistry* 1996, 35, 4079–4083.
- Boudker, O.; Todd, M. J.; Freire, E. *J Mol Biol* 1997, 272, 770–779.
- Guidry, J. J.; Wittung-Stafshede, P. *Arch Biochem Biophys* 2002, 405, 280–282.
- Fossati, G.; Lucietto, P.; Giuliani, P.; Coates, A. R.; Harding, S.; Colfen, H.; Legname, G.; Chan, E.; Zaliani, A.; Mascagni, P. *J Biol Chem* 1995, 270, 26159–26167.
- Galli, G.; Ghezzi, P.; Mascagni, P.; Marcucci, F.; Fratelli, M. *In Vitro Cell Dev Biol Anim* 1996, 32, 446–450.
- Higurashi, T.; Nosaka, K.; Mizobata, T.; Nagai, J.; Kawata, Y. *J Mol Biol* 1999, 291, 703–713.
- Lucietto, P.; Fossati, G.; Ball, H. L.; Giuliani, P.; Mascagni, P. *J Pept Res* 1997, 49, 308–323.
- Mascagni, P.; Ball, H. L.; Bertolini, G. *Anal Chim Acta* 1997, 352, 375–385.
- Harding, S. E.; Horton, J. C.; and Morgan P. J. *Analytical Ultracentrifugation in Biochemistry and Polymer Science*; Harding, S. E.; Rowe, A. J.; Horton, J. C., Eds.; R. Soc. Chem.: Cambridge, 1992.
- Harding, S. E.; Horton, J. C.; Colfen H. *Eur Biophys J* 1997, 25, 347–359.
- Laue, T. M.; Shah, B. D.; Ridgeway, T. M.; Pelletier, S. L. *Analytical Ultracentrifugation in Biochemistry and Polymer Science*; Harding, S. E.; Rowe, A. J.; Horton J.C. Eds; R. Soc. Chem.: Cambridge, 1992.
- Taneja, B.; Mande, S. C. *Protein Eng* 2001, 14, 391–395.
- Mande, S. C.; Mehra, V.; Bloom, B. R.; Hol, W. G. *Science* 1996, 271, 203–207.

43. Landry, S. J.; Zeilstra-Ryalls, J.; Fayet, O.; Georgopoulos, C.; Gierasch, L. M. *Nature* 1993, 364, 255–258.
44. Soltys, B. J.; Gupta, R. S. *Cell Biol Int* 1997, 21, 315–320.
45. Chan, E.; Fossati, G.; Giuliani, P.; Lucietto, P.; Zaliani, A.; Coates, A. R. M.; Mascagni, P. *Biochem Biophys Res Commun* 1995, 211, 14–20.
46. Privalov, P. L. *Crit Rev Biochem Mol Biol* 1990, 25, 281–305.
47. Brandts, J. F. *J Am Chem Soc* 1964, 86, 4291–4301.
48. Kumarevel, T. S.; Gromiha, M. M.; Ponnuswamy, M. N. *Biophys Chem* 1998, 75, 105–113.
49. Fields, P. A. *Comp. Biochem Physiol A* 2001, 129, 417–431.
50. Imagawa, K.; Numata, Y.; Katsuura, G.; Sakaguchi, I.; Morita, A.; Kikuoka, S.; Matumoto, Y.; Tsuji, T.; Tamaki, M.; Sasakura, K.; Teraoka, H.; Hosoda, K.; Ogawa, Y.; Nakao, K. *J Biol Chem* 1998, 273, 35245–35249.
51. Santos-Alvarez, J.; Goberna, R.; Sanchez-Margalet, V. *Cell Immunol* 1999, 194, 6–11.
52. Ranford, J. C.; Henderson, B. *Mol Pathol* 2002, 55, 209–213.
53. Qian, N.; Sejnowski, T. J. *J Mol Biol* 1988, 202, 865–884.
54. Garnier, J.; Osguthorpe, D. J.; Robson, B. *J Mol Biol* 1978, 120, 97–120.
55. Maxfield, F. R.; Scheraga, H. A. *Biochemistry* 1979, 18, 697–704.

Reviewing Editor: Dr. Murray Goodman